Astroparticle Physics 2919/20

Lectures:

http://particle.astro.ru.nl/goto.html?astropart1920

lecture 4
Electromagnetic cascades

Gaisser chapter 15

15   Electromagnetic cascades

Extensive Air Shower

Proton 10^{15} eV:
on ground
10^6 particles
80% photons
18% electr./positr.
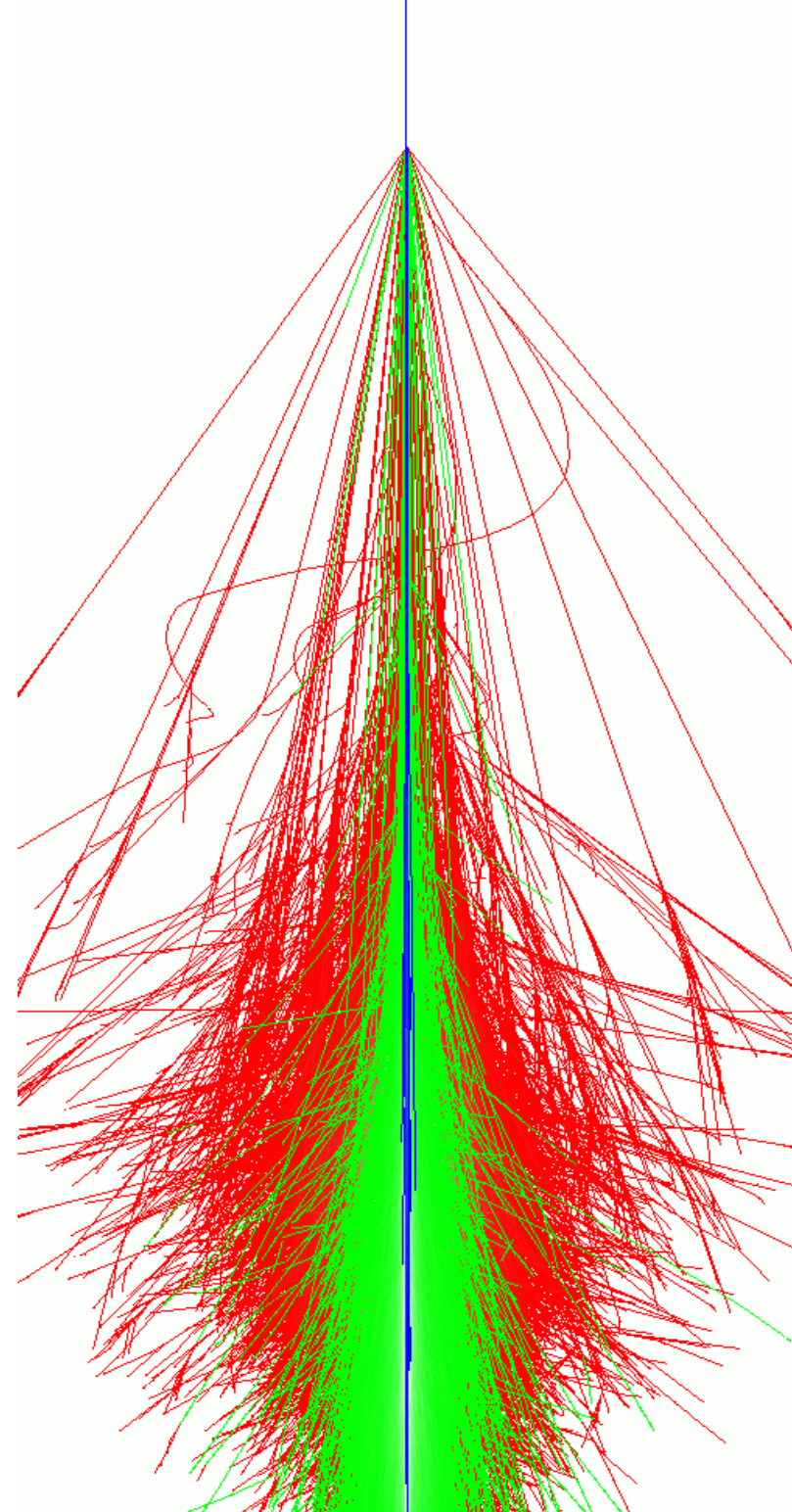**1.7% muons**
0.3% hadrons
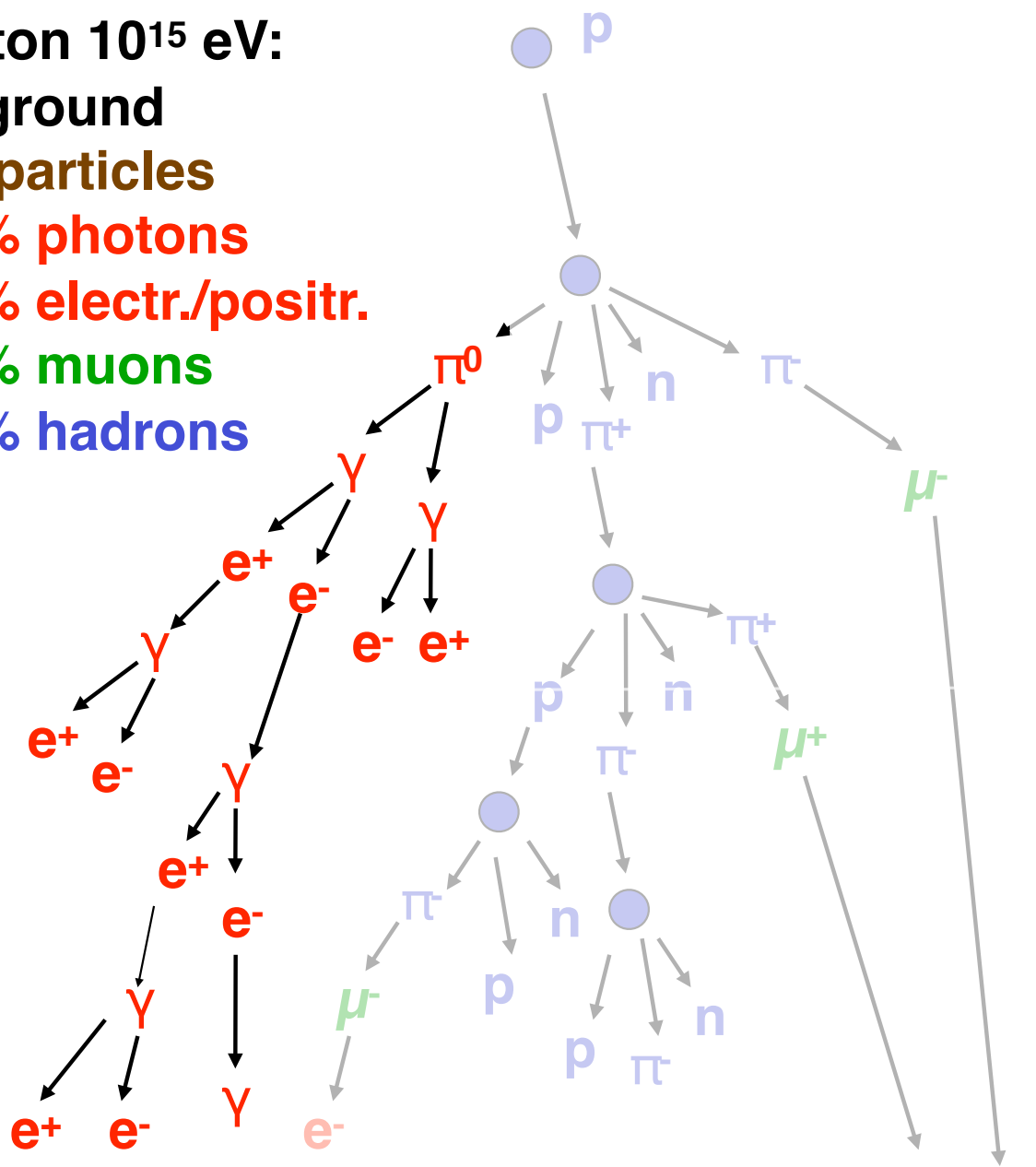
electromagnetic   **hadronic**   **muonic**

shower component

The evolution of the number and energy spectra of photons and electrons in an air shower initiated by a single electron or photon incident at the top of the atmosphere is governed by the coupled equations (5.25 and 5.26) introduced earlier. In Chapter 5 we discussed solutions subject to power-law boundary conditions. For an air shower, the same equations have to be solved subject to an appropriate δ-function boundary condition at $t = 0$. The standard approach is a Monte Carlo computer code, such as GEANT [191] or EGS [192]. To give insight into the basic structure of electromagnetic cascades, as well as for historical perspective, we devote this chapter to a discussion of approximate formulas that contain the essential physics and set the stage for the discussion of more complicated hadronic cascades in the next chapter.

$$\frac{d\gamma}{dt} = -\frac{\gamma}{\lambda_{\text{pair}}} + \int_0^1 \pi\left(\frac{W}{v}, t\right)\phi(v)\frac{dv}{v} \tag{5.25}$$

and

$$\frac{d\pi}{dt} = -\frac{\pi}{\lambda_{\text{brems}}} + \int_0^1 \pi\left(\frac{E}{1-v}, t\right)\phi(v)\frac{dv}{1-v} + 2\int_0^1 \gamma\left(\frac{E}{u}, t\right)\psi(u)\frac{du}{u}. \tag{5.26}$$

The first two terms on the right side of Eq. 5.26 must be combined (using the relation 5.19) to remove the infrared divergence at $v \to 0$.

A Matthews Heitler Model – Electromagnetic Cascades
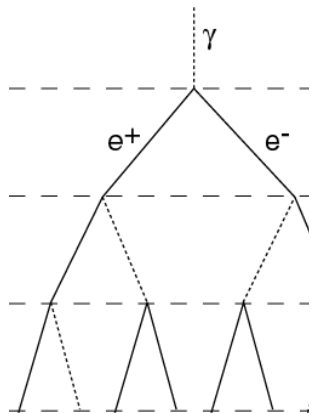
pair production $\gamma \rightarrow e^+ + e^-$

bremsstrahlung $e \rightarrow e + \gamma$

splitting length $d = X_0 \ln 2$

radiation length $X_0 = 36.7$ g/cm²

A Heitler model of extensive air showers

J. Matthews *

Department of Physics and Astronomy, Louisiana State University, Baton Rouge, LA 70803, USA
Department of Physics, Southern University, Baton Rouge, LA 70813, USA

after *n* splitting lengths: $\quad x = n X_0 \ln 2 \quad$ **and** $\quad N = 2^n = \exp\left(\dfrac{x}{X_0}\right)$

energy per particle $\quad E = E_0/N \qquad$ **critical energy** $\quad E_c^e = 85$ MeV

number of particles at shower maximum

$$N_{max} = 2^{n_c} = \frac{E_0}{E_c^e} \qquad n_c = \frac{\ln\left(\frac{E_0}{E_c^e}\right)}{\ln 2}$$

J. Matthews, Astrop. Phys. 22 (2005) 387

JRH, Mod. Phys. Lett. A 22 (2007) 1533

Jörg R. Hörandel, APP 2019/20   5

A Matthews Heitler Model – Electromagnetic Cascades
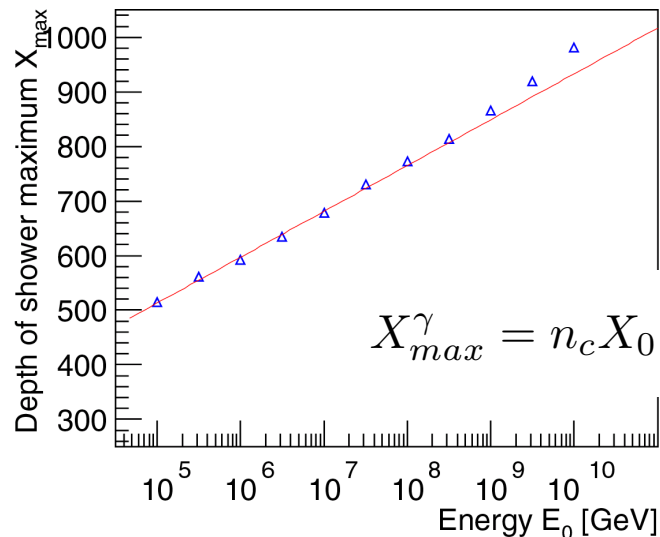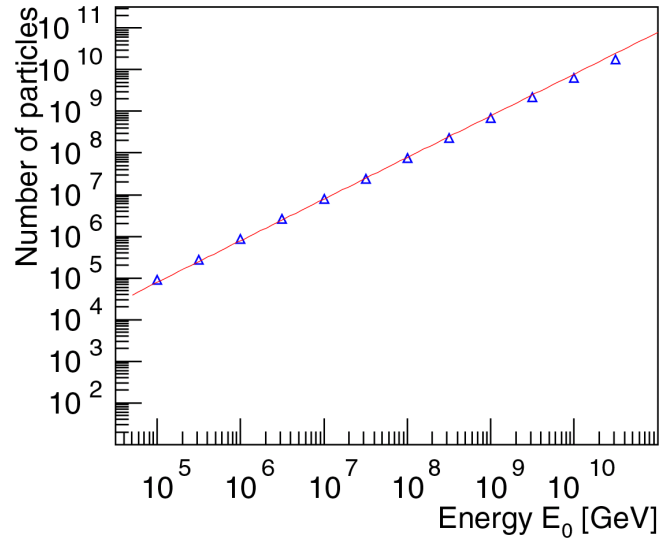
number of electrons at shower maximum

$$N_e^{max} = \frac{E_0}{gE_c^e} \approx 9.0 \cdot 10^5 \frac{E_0}{\text{PeV}} \qquad g \approx 13$$
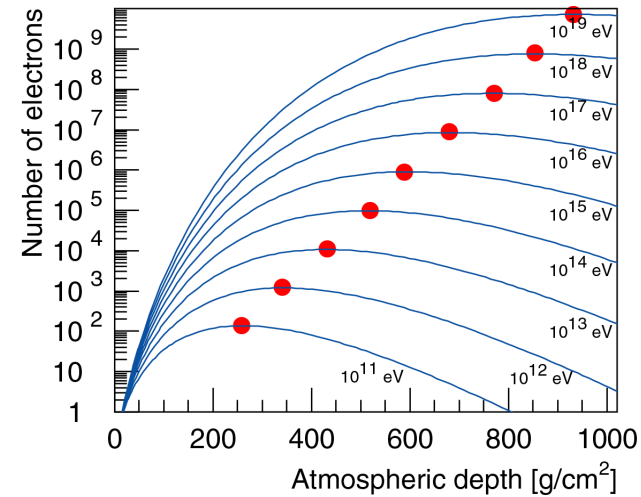
depth of shower maximum

$$X_{max}^\gamma = n_c X_0 \ln 2 = X_0 \ln\left(\frac{E_0}{E_c^e}\right) \approx 597 \frac{\text{g}}{\text{cm}^2} + 84 \frac{\text{g}}{\text{cm}^2} \lg\left(\frac{E_0}{\text{PeV}}\right)$$

The basic features of Eqs. 15.1 and 15.2 hold for high-energy electromagnetic cascades and also, approximately, for hadronic cascades; namely

$$N_{max} \propto E_0 \quad \text{and} \quad X_{max} \propto \ln(E_0). \tag{15.3}$$

15.1.2 General form of solution

In general, the particle content of any air shower (number of particles of each species as a function of E and X) is given by the solution of the coupled cascade equations (5.1) subject to the delta function boundary condition (Eq. 5.9). If the transfer functions, F_{ji} scale (Eq. 5.4), then there is no dimensional quantity in the problem and the dimensionless quantity, $E_i N_i(E_i, E_0, X)$ must be a function only of the ratio $\xi_i \equiv E_i/E_0$. Let us call this dimensionless function

$$\mathcal{F}_i(\xi_i, X) \equiv E_i N_i(E_i, E_0, X). \tag{15.4}$$

The yield function, $\mathcal{F}_i$, gives the number of particles of type i per logarithmic interval of fractional energy. The yield depends only on the ratio of the particle energy, E_i, to the total energy, E_0, of the air shower. This result holds only to the extent that scaling is valid and only when decay and continuous energy loss can be neglected. It is approximately valid for high-energy hadrons and for electrons and photons with $E > E_c$ in air showers.

5.1 Basic equation and boundary conditions

The linear development of a cascade of particles in the atmosphere can be described by a system of equations of the form

$$\frac{\mathrm{d}N_i(E_i, X)}{\mathrm{d}X} = -\frac{N_i(E_i, X)}{\lambda_i} - \frac{N_i(E_i, X)}{d_i}$$
$$+ \sum_{j=i}^{J} \int_{E}^{\infty} \frac{F_{ji}(E_i, E_j)}{E_i} \frac{N_j(E_j, X)}{\lambda_j} \mathrm{d}E_j. \tag{5.1}$$

Here, $N_i(E_i, X)\mathrm{d}E_i$ is the flux of particles of type i at slant depth X in the atmosphere with energies in the interval E to $E + \mathrm{d}E$. Note that X is measured from the top of the atmosphere downward along the direction of the particle that initiated the cascade, as shown in Figure 5.1. The probability that a particle of type j interacts in traversing an infinitesimal element of the atmosphere is $\mathrm{d}X/\lambda_j(E_j)$, where λ_j is the interaction length in air of particles of type j. Similarly, $\mathrm{d}X/d_j(E_j)$ is the probability that a particle of type j decays in $\mathrm{d}X$. All three quantities X, λ_j and d_j must be expressed in consistent units, and we use g/cm^2. Energy loss by ionization is not included in Eq. 5.1 because it is not important for hadrons in the atmosphere or for high-energy electrons.

5.2 Boundary conditions

We will need solutions of the cascade equation 5.1 subject to two physically important boundary conditions that correspond to two quite different types of experiments. The boundary conditions are

$$N(E, 0) = N_0(E) = \frac{dN}{dE} \approx 1.7\, E^{-2.7}\, \frac{\text{nucleons}}{\text{cm}^2\, \text{sr}\, \text{s}\, \text{GeV}/A} \qquad (5.8)$$

and

$$N(E, 0) = A\, \delta(E - \frac{E_0}{A})\, \delta(t - t_0), \qquad (5.9)$$

air shower

where A here is the mass number of an incident nucleus. Eq. 5.8 is relevant for a detector that simply measures the rate at which particles of a given type pass through. The explicit power law approximation is based on data with primary energy less than a TeV, but it is useful as a guide up to a PeV. Eq. 5.9 is the boundary condition relevant for an air shower experiment that traces the development of a cascade through the atmosphere. An example is an array of detectors on the ground with a fast-timing capability that can be triggered to measure the coincident, extended shower front initiated at the top of the atmosphere by a single particle. In the case of a ground array, the primary particle has to have sufficient energy to give a measurable cascade at the surface of the Earth. Cherenkov and fluorescence detectors can trace the development of showers through the atmosphere.

The function $F_{ji}(E_i, E_j)$ in Eq. 5.1 is the dimensionless particle yield that follows from the inclusive cross section (integrated over transverse momentum) for a particle of energy E_j to collide with an air nucleus and produce an outgoing particle i with energy $E_i < E_j$. In general, we define

$$F_{ji}(E_i, E_j) \equiv E_i \frac{1}{\sigma_j^{\text{air}}} \frac{\mathrm{d}\sigma_{j\,\text{air}\to i}}{\mathrm{d}E_i} = E_i \frac{\mathrm{d}n_i(E_i, E_j)}{\mathrm{d}E_i}, \qquad (5.4)$$

where $\mathrm{d}n_i$ is the number of particles of type i produced on average in the energy bin $\mathrm{d}E_i$ around E_i per collision of an incident particle of type j. All quantities in Eq. 5.4 are defined in the lab system. The relation to center-of-mass quantities can be derived from the definitions in Table 4.1. From Eq. 4.15 it follows that for energetic secondaries, i.e. those with $E_c \gg m_{T,c}$

$$E_c/E_a = x_L \approx x^*. \qquad (5.5)$$

(We always define CMS as a projectile on a target *nucleon* even when that nucleon is bound in a nucleus, because nuclear binding energies will usually be much lower than energies of interest in cosmic ray problems we consider.)

It is interesting to express the differential flux, $N_i(E_i, X)$, that results from a spectrum of primary particles in terms of $\mathcal{F}$. It is

$$N_i(E_i, X) = \int_0^1 N_0(E_i/\xi_i)\, \mathcal{F}(\xi_i, X)\, \mathrm{d}\xi_i,\tag{15.5}$$

where $N_0(E_0)$ is the differential spectrum of primary particles. For a power law spectrum, $N_0(E_0) \propto E^{-(\gamma+1)}$ and

$$N_i(E_i, X) = N_0(E_i) \int_0^1 \xi_i^{\gamma-1}\, \mathcal{F}(\xi_i, X)\, \mathrm{d}\xi_i.\tag{15.6}$$

Note the similarity between the role of a whole cascade (represented here by $\mathcal{F}$) and the role of individual interactions in the spectrum weighted moments given by Eq. 5.48. The integral in Eq. 15.6 is a spectrum weighted moment of a whole cascade. In fact, in the late 1940 it was not clear experimentally whether elementary multiple production occurs at all or whether events with more than one created pion required interactions of the projectile with several separate target nucleons inside a nucleus. This is the question of "multiple" *versus* "plural" production discussed by Heitler and others in Volume **21** of Reviews of Modern Physics, 1949.

In general, the spectrum-weighted moments of the inclusive cross sections $j + \text{air} \rightarrow i$,

$$Z_{ji} \equiv \int_0^1 (x_L)^{\gamma-1} F_{ji}(x_L)\, dx_L, \qquad (5.48)$$

determine the uncorrelated fluxes of energetic particles in the atmosphere [197, 198]. For $\gamma = 1$, it follows from Eq. 5.4 that $Z_{ji}(1)$ is simply the average fraction of the interaction energy that goes into particles of type i in interactions of particles of type j. For $\gamma > 1$ the contribution to the moment from $x_L \rightarrow 0$ vanishes. Thus, for a steep primary spectrum, the uncorrelated fluxes depend on the behavior of the inclusive cross sections only in the forward fragmentation region ($x^* > 0$ in Eqs. 4.15 and 5.5). This is why the μ^+/μ^- ratio remains large and greater than 1, which we will discuss in Chapter 6. It is also why Approximation A remains useful for uncorrelated fluxes of energetic particles, because hadronic scaling (Eq. 5.45) is more nearly valid in the fragmentation regions than elsewhere.

For later reference, we give here a table (Table 5.2) of spectrum-weighted moments.[4] This table is analogous to the Table 5.1 for electrons and photons. The Z-factors from Ref. [199] are tabulated for $\gamma = 1$, $\gamma = 1.7$ and $\gamma = 2.0$. For comparison, we also show the Z-factors at $\gamma = 1.7$ for the first edition of this book [200] and for a new version of Sibyll [155]. Since the primary spectrum is not a perfect power-law over the whole energy region, it is also important to see how the Z-factors depend on spectral index. This is shown in Figure 5.2 for integral spectral indexes between $\gamma = 1$ (momentum fraction) and $\gamma = 2.4$ (above the knee).

15.2 Analytic solutions in cascade theory

The coupled cascade equations for photons (Eq. 5.20) and electrons (Eq. 5.21) are given in Chapter 5. They depend on particle energy and distance expressed as $t = X(\mathrm{g/cm^2})/X_0$. For air the radiation length is $X_0 \approx 37 \ \mathrm{g/cm^2}$. Analytic forms for solutions of the electromagnetic cascade equations subject to power law boundary conditions were presented in Chapter 5. Here we discuss the relation of the power-law forms to the corresponding solutions of the same equations subject to delta-function boundary conditions.

The paradigm for parametrizations of air showers (hadronic as well as electromagnetic) is the work on electromagnetic cascades summarized in the 1941 review by Rossi & Greisen [194]. Since the details are available in their paper and in Rossi's 1952 book [498], we will outline the results here as briefly as possible consistent with motivating the forms of the parametrizations and summarizing their essential features. The same approach can be used for hadronic air showers, as we note in the following chapter.

5.4.1 Cascade equations

The coupled equations for electromagnetic cascades are an instance of Eq. 5.1. They are

$$\frac{d\gamma}{dt} = -\frac{\gamma(W,t)}{\lambda_{\text{pair}}} + \int_W^\infty \pi(E',t) \frac{dn_{e\to\gamma}}{dWdt} dE' \qquad (5.20)$$

and

$$\frac{d\pi}{dt} = -\frac{\pi(E,t)}{\lambda_{\text{brems}}} + \int_E^\infty \pi(E',t) \frac{dn_{e\to e}}{dEdt} dE'$$
$$+ 2\int_E^\infty \gamma(W',t) \frac{dn_{\gamma\to e}}{dEdt} dW', \qquad (5.21)$$

where $\gamma(W,t)dW$ is the number of photons in dW at depth t and $\pi(E,t)dE$ is the number of $e^\pm$ in dE at depth t. For energies that are large compared to the critical energy, collisional losses and Coulomb scattering can be neglected and the scaling functions 5.13 and 5.16 can be used. This is *Approximation A*.

The starting point is to show that the Mellin transforms of $\gamma(W, t)$ and $\pi(E, t)$ satisfy the same parametric equations (5.30, 5.31) as the coefficients $f_\gamma(t)$ and $f_\pi(t)$ that enter the solutions for power-law boundary conditions derived in Chapter 5. This is done by taking the Mellin transform of Eqs. 5.25 and 5.26. The Mellin transform of a function $F(W)$ is defined as

$$\mathcal{M}_F(s) \equiv \int_0^\infty W^s F(W) \mathrm{d}W. \tag{15.7}$$

Transforming the last term of Eq. 5.25, for example, involves calculating

$$\int_0^\infty W^s \int_0^1 \frac{\mathrm{d}v}{v} \pi(\frac{W}{v}, t)\phi(v)\mathrm{d}W = \int_0^1 \mathrm{d}v\phi(v)v^s \mathcal{M}_\pi(s, t) = C(s)\mathcal{M}_\pi(s, t). \tag{15.8}$$

Given the correspondence $\mathcal{M}_\pi(s, t) \sim f_\pi(t)$ and $\mathcal{M}_\gamma(s, t) \sim f_\gamma(t)$, the same analysis in terms of elementary solutions of the form $\mathcal{M}(s, t) \propto \exp(\lambda t)$ as in Eqs. 5.32 to 5.35 applies. ($C(s)$ and other relevant functions are given in Table 5.1.) For a cascade generated by a single photon of energy W_0 the boundary conditions are $f_\gamma(0) = \mathcal{M}_\gamma(0) = (W_0)^s$ and $\mathcal{M}_\pi(0) = 0$, which follow from $\gamma(0) = \delta(W - W_0)$ and $\pi(0) = 0$. For a single incident electron of energy E_0, the conditions are $\mathcal{M}_\gamma(0) = 0$ and $\mathcal{M}_\pi(0) = (E_0)^s$.

Table 5.1 gives some values for the spectrum-weighted moments and other parameters of electromagnetic cascade theory in the conventional notation of [194]. In terms of these definitions, Eqs. 5.28 and 5.29 may be rewritten as

$$\left[\frac{d}{dt} + \sigma_0\right] f_\gamma(t) - C(s) f_\pi(t) = 0 \tag{5.30}$$

and

$$\left[\frac{d}{dt} + A(s)\right] f_\pi(t) - B(s) f_\gamma(t) = 0. \tag{5.31}$$

By solving Eq. 5.30 for f_π and substituting the result into Eq. 5.31 we get a second order differential equation for f_π. Similarly, substituting f_γ from Eq. 5.31 into Eq. 5.30, we get the equation for f_γ. Both $f_\pi(t)$ and $f_\gamma(t)$ satisfy the same second order differential equation,

$$f'' + (A + \sigma_0) f' + (A\sigma_0 - BC) f = 0, \tag{5.32}$$

which has *elementary solutions* of the form $f \propto \exp(\lambda t)$, where $\lambda(s)$ satisfies the quadratic equation obtained by substitution of the exponential form into Eq. 5.32,

$$\lambda^2 + (A + \sigma_0) \lambda + (A\sigma_0 - BC) = 0. \tag{5.33}$$

This is *Approximation A*. With the identifications,

$$E' \frac{\mathrm{d}n_{e \to \gamma}}{\mathrm{d}W \mathrm{d}t} = \phi\left(\frac{W}{E'}\right), \quad (5.22)$$

$$W' \frac{\mathrm{d}n_{\gamma \to e}}{\mathrm{d}E \mathrm{d}t} = \psi\left(\frac{E}{W'}\right) \quad (5.23)$$

and

$$E' \frac{\mathrm{d}n_{e \to e}}{\mathrm{d}E \mathrm{d}t} = \phi\left(1 - \frac{E}{E'}\right), \quad (5.24)$$

the cascade equations 5.20 and 5.21 can be written in scaling form:

$$\frac{\mathrm{d}\gamma}{\mathrm{d}t} = -\frac{\gamma}{\lambda_{\mathrm{pair}}} + \int_0^1 \pi\left(\frac{W}{v}, t\right) \phi(v) \frac{\mathrm{d}v}{v} \quad (5.25)$$

and

$$\frac{\mathrm{d}\pi}{\mathrm{d}t} = -\frac{\pi}{\lambda_{\mathrm{brems}}} + \int_0^1 \pi\left(\frac{E}{1-v}, t\right) \phi(v) \frac{\mathrm{d}v}{1-v} + 2 \int_0^1 \gamma\left(\frac{E}{u}, t\right) \psi(u) \frac{\mathrm{d}u}{u}. \quad (5.26)$$

The first two terms on the right side of Eq. 5.26 must be combined (using the relation 5.19) to remove the infrared divergence at $v \to 0$.

The air shower solutions are then obtained by inverting the Mellin transforms,

$$\gamma(W, t) = \frac{1}{2\pi i} \int_{-i\infty+s_0}^{i\infty+s_0} W^{-(s+1)} f_\gamma(s, t) ds,$$ (15.9)

for photons, with a similar expression for electrons. Solutions subject to δ-function boundary conditions are thus convolutions of the elementary solutions for power law boundary conditions.

It is only in the inversion of the Mellin transforms that approximations are required to obtain analytic solutions. The approximation consists of evaluating Eq. 15.9 by the saddle point method. To simplify the formulas and to motivate the standard parametrizations it is also useful to make some numerical approximations to the Mellin transform functions. The function $\lambda_1(s)$ is positive for $s < 1$ and negative for $s > 1$. An approximation that is good to better than 2% for $0.5 \leqslant s \leqslant 2$ is

$$\lambda_1(s) = \frac{1}{2}(s - 1 - 3\ln s).$$ (15.10)

The other root of Eq. 5.33 ($\lambda_2(s)$) is always negative and larger in magnitude than $\lambda_1(s)$, so that only the term with λ_1 is important for $t \gg 1$.

As specific examples we consider the solutions for electrons plus positrons for a single incident photon of energy W_0 and for a single incident electron of $E_0 = W_0$. From Eq. 5.36 the Mellin transform for an incident photon is

$$f_\pi^{(\gamma)}(s,t) \approx \frac{B(s)}{\lambda_1(s) - \lambda_2(s)}(W_0)^s \exp[\lambda_1(s)t]. \qquad (15.11)$$

The corresponding expression for an incident electron is

$$f_\pi^{(e^\pm)}(s,t) \approx \frac{\sigma_0 + \lambda_1(s)}{\lambda_1(s) - \lambda_2(s)}(E_0)^s \exp[\lambda_1(s)t]. \qquad (15.12)$$

The inverse transform of $f_\pi^{(\gamma)}(s,t)$, for example, gives

$$\pi^{(\gamma)}(E,t)\mathrm{d}E = \frac{\mathrm{d}E}{E}\frac{1}{2\pi i}\int_{-i\infty+s_0}^{i\infty+s_0}\left\{\frac{B(s)}{\sqrt{s}[\lambda_1(s) - \lambda_2(s)]}\right\} \qquad (15.13)$$
$$\times\sqrt{s}\left(\frac{W_0}{E}\right)^s \exp[\lambda_1(s)t]\mathrm{d}s,$$

which can be rewritten as

$$\pi^{(\gamma)}(E,t)\mathrm{d}E = \frac{\mathrm{d}E}{E}\frac{1}{2\pi i}\int_{-i\infty+s_0}^{i\infty+s_0}\left\{\frac{B(s)}{\sqrt{s}[\lambda_1(s) - \lambda_2(s)]}\right\} \qquad (15.14)$$
$$\times \exp[\lambda_1(s)t + sy + \frac{1}{2}\ln s]\mathrm{d}s.$$

Here $y \equiv \ln(E_0/E)^1$ (a quantity called "lethargy" in the context of radiation shielding). The factors in curly brackets have been arranged to cancel a $1/\sqrt{s}$ behavior of $\lambda_1(s) - \lambda_2(s)$ at small s. The rapidly varying part of the s-dependence in the integrand is thus all in the argument of the exponent.

The roots of Eq. 5.33 are

$$2\lambda_1(s) = -[A(s) + \sigma_0] + \{[A(s) - \sigma_0]^2 + 4B(s)C(s)\}^{\frac{1}{2}} \qquad (5.34)$$

and

$$2\lambda_2(s) = -[A(s) + \sigma_0] - \{[A(s) - \sigma_0]^2 + 4B(s)C(s)\}^{\frac{1}{2}}. \qquad (5.35)$$

The solutions, $f_\gamma(t)$ and $f_\pi(t)$, are linear combinations of the elementary solutions $\exp[\lambda_1 t]$ and $\exp[\lambda_2 t]$ appropriate for the boundary conditions at injection. For example, for a power-law distribution of injected photons with $\gamma(W,0) = f_\gamma(0)W^{-(s+1)}$ at the top of the atmosphere,

$$f_\pi(t) = \frac{Bf_\gamma(0)}{\lambda_1 - \lambda_2}\left\{e^{\lambda_1 t} - e^{\lambda_2 t}\right\} \qquad (5.36)$$

and

$$f_\gamma(t) = \frac{f_\gamma(0)}{\lambda_1 - \lambda_2}\left\{(A + \lambda_1)e^{\lambda_1 t} - (A + \lambda_2)e^{\lambda_2 t}\right\}. \qquad (5.37)$$

Thus, for a spectrum of injected photons with integral spectral index γ and no injected electrons, the differential spectrum of photons plus electrons and positrons at depth t is

$$\frac{dN_{\gamma + e\pm}}{dE} = \frac{f_\gamma(0)}{\lambda_1 - \lambda_2}E^{-(\gamma+1)}\left\{(A + B + \lambda_1)e^{\lambda_1 t} - (A + B + \lambda_2)e^{\lambda_2 t}\right\}. \qquad (5.38)$$

The saddle point approximation for the integral in Eq. 15.14 consists of expanding the argument of the exponent to second order in a Taylor series about $\bar{s}$, where $\bar{s}$ is the solution of

$$\frac{d}{ds}\left[\lambda_1(s)t + sy + \frac{1}{2}\ln s\right] = 0.$$

The slowly varying part of the integrand in curly brackets is approximated by its value at $s = \bar{s}$. This leaves a Gaussian integral which can be evaluated by integrating along the contour through the saddle point at $\bar{s}$.

The same procedure can be carried out to find the corresponding approximation for electrons generated by an incident electron and for photons in showers of either type. Integral spectra also have the same form. (From Eq. 15.13 it is apparent that integral spectra differ from the corresponding differential spectra by an extra factor of $1/s$ in the integrand.) In general, the integral to be approximated is of the form

$$I(t, \bar{s}) = \frac{1}{2\pi i}\int_{-i\infty+\bar{s}}^{i\infty+\bar{s}} ds\ \{F(s)\}\exp[\lambda_1(s)t + sy - n\ln s], \qquad (15.15)$$

where n is given in Table 15.1. The condition for the location of the extremum is

$$\lambda_1'(\bar{s})t + y - \frac{n}{\bar{s}} = 0. \qquad (15.16)$$

Table 15.1 *Quantities in the Rossi & Greisen approximations.*

	n	$F(s)$
$e^+ + e^-$ from γ	$-\dfrac{1}{2}$	$\dfrac{B(s)}{\sqrt{s}\,[\lambda_1(s)-\lambda_2(s)]}$
$e^+ + e^-$ from $e^{\pm}$	0	$\dfrac{\sigma_0+\lambda_1(s)}{\lambda_1(s)-\lambda_2(s)}$
γ from γ	0	$-\dfrac{\sigma_0+\lambda_2(s)}{\lambda_1(s)-\lambda_2(s)}$
γ from $e^{\pm}$	$+\dfrac{1}{2}$	$\dfrac{\sqrt{s}\,C(s)}{\lambda_1(s)-\lambda_2(s)}$

Expanding the argument of the integrand about $\bar{s}$ gives

$$I(t,\bar{s}) \approx F(\bar{s}) \exp[\lambda_1(\bar{s})t + \bar{s}y - n \ln \bar{s}]$$

$$\times \frac{1}{2\pi i} \int_{-i\infty+\bar{s}}^{i\infty+\bar{s}} ds \, \exp[(\lambda_1''(s)t + n/\bar{s}^2)\frac{(s-\bar{s})^2}{2}]$$

$$\approx \frac{F(\bar{s})}{\sqrt{\lambda_1''(s)t + n/\bar{s}^2}} \frac{\exp[\lambda_1(\bar{s})t + \bar{s}y - n \ln \bar{s}]}{\sqrt{2\pi}}. \qquad (15.17)$$

The depth of maximum, T_{max}, occurs approximately when the argument of the exponential is a maximum,

$$\left\{ \frac{d}{ds}[\lambda_1(s)t + sy - n \ln s] \right\} \frac{ds}{dt} + \lambda_1(s) = \lambda_1(s) = 0. \qquad (15.18)$$

(In this equation and below, the bar over s is understood.) The factor in square brackets vanishes by Eq. 15.16, and $\lambda_1(s) = 0$ for $s = 1$. It therefore follows from Eq. 15.16 that $T_{\text{max}} = -(y-n)/\lambda_1'(1)$. With the approximation 15.10, $\lambda_1'(1) \approx -1$ and

$$T_{\text{max}} \approx \ln \frac{E_0}{E} - n. \qquad (15.19)$$

Here T_{max} is explicitly a function of E and is shallower for higher E as expected in a cascade. Values of n and $F(s)$ are listed in Table 15.1 for the differential spectra. For each case the corresponding integral expression is the same except that

$$n(\text{integral}) = n(\text{differential}) + 1.$$

Note that maximum is reached one-half radiation length sooner for showers initiated by electrons than for photon-initiated showers.

The parameter s, related to t and y by Eq. 15.16, is called the *age parameter*. Since $I(t) \propto \exp[\lambda_1(s) t]$, the number of shower particles in a given energy range increases with depth for $s < 1$ (i.e. when $\lambda_1(s)$ is positive), reaches a maximum when $s = 1$, and declines for $s > 1$ (when $\lambda_1(s)$ is negative). With the approximation of Eq. 15.10,

$$s = \frac{2n + 3t}{t + 2y},$$ (15.20)

and

$$\lambda_1''(s) \sim 1.5/s^2.$$ (15.21)

From Eqs. 15.14 and 15.17 one can see that in general the energy spectrum of particles in a shower will be of the form

$$\frac{dN}{dE} = \frac{1}{E_0} \left(\frac{E_0}{E}\right)^{s+1} \exp[\lambda_1(s) t] \times (\text{function of } s).$$ (15.22)

Since s depends only logarithmically on $y = \ln(E_0/E)$, the energy dependence is approximately a power. The spectrum steepens as age increases – physically, high-energy particles become rare as the shower develops. At maximum $s = 1$, and the spectrum is $\sim E^{-2}$. (Note that because s does depend on y, these statements apply only for limited ranges of energy.)

Approximations like Eq. 15.17 are used with s as a parameter. For each value of s one finds the corresponding t from Eq. 15.16. The value of $I(t(s), s)$ is then plotted at this value of t. With the help of Eqs. 15.10 and 15.20, the exponent in Eq. 15.17 can be written in the following conventional form:

$$\exp\left[\lambda_1(s)t + sy - n\ln s\right] = \exp\left[n(1 - \ln s) + t\left(1 - \frac{3}{2}\ln s\right)\right]. \qquad (15.23)$$

Explicitly, for example for the integral spectra,

$$\Pi^{(e^\pm)}(> E, t) \approx \frac{1}{(\sqrt{2\pi})^{1/2}} \frac{\sigma_0 + \lambda_1(s)}{\lambda_1(s) - \lambda_2(s)} \frac{e}{\sqrt{1.5t + 1}} \exp\left[t\left(1 - \frac{3}{2}\ln s\right)\right] \qquad (15.24)$$

and

$$\Pi^{(\gamma)}(> E, t) \approx \frac{1}{(\sqrt{2\pi})^{1/2}} \frac{B(s)}{\sqrt{s}[\lambda_1(s) - \lambda_2(s)]} \frac{\sqrt{s}\, e^{\frac{1}{2}}}{\sqrt{1.5t + 0.5}} \exp\left[t\left(1 - \frac{3}{2}\ln s\right)\right] \qquad (15.25)$$

At maximum $T_{\max} = \ln(E_0/E) - n$, and $s = 1$, so[2]

$$\Pi^{(e^\pm)}(> E, t) \approx \frac{0.14}{\sqrt{\ln(E_0/E) - 0.33}} \frac{E_0}{E} \qquad (15.26)$$

and

$$\Pi^{(\gamma)}(> E, t) \approx \frac{0.14}{\sqrt{\ln(E_0/E) - 0.25}} \frac{E_0}{E}. \qquad (15.27)$$

Note the similarity of the formulas for depth of maximum (Eq. 15.19) and size at maximum (Eqs. 15.26 and 15.27) here as compared with those obtained above with the simple Heitler branching model (Eqs. 15.2 and 15.1).

15.3 Approximations for total number of particles

What is measured by a scintillator that samples an air shower front is the signal produced by all the electrons and positrons incident on the scintillator plus the signal produced by photons that convert in the scintillator.[3] One would therefore like a formula for the total number of electrons and positrons down to, say, 20 MeV. Energy loss and Coulomb scattering must be taken into account, and Approximation A is no longer adequate. The conventional form used for the total number of electrons in a photon-initiated shower of energy E_0 is (Greisen, 1956) [499]

$$N(t) \sim \frac{0.31}{(\beta_0)^{1/2}} \exp[t(1 - \frac{3}{2}\ln s)], \qquad (15.28)$$

where $\beta_0 = \ln(E_0/E_c)$ and s, t and $y = \beta_0$ are related by Eq. 15.20 with $n = 0$. This simple expression is similar in form to the Approximation A solutions, but has a depth of maximum that depends on the critical energy rather than energy of the photon.

The approximation 15.28 is plotted in Figure 15.2 to illustrate how showers evolve over a wide range of primary energy. Shower maximum occurs for $s = 1$. Therefore from Eq. 15.20 with $n = 0$,

$$X_{\max}^{(\mathrm{em})} = X_0 T_{\max} = X_0 \ln \left(\frac{E_0}{E_c} \right) \qquad (15.29)$$

and

$$N_{\max}^{(\mathrm{em})} = \frac{0.31}{\sqrt{\ln(E_0/E_c)}} \frac{E_0}{E_c} \sim 10^6 \left(\frac{E_0(\mathrm{GeV})}{10^6} \right). \qquad (15.30)$$

Analogous relations for charged particles in hadron-induced showers will be discussed in the following chapter.

Figure 15.2 shows how Eq. 15.28 for electromagnetic cascades evolves over a wide range of primary photon energy. Similar relations among shower age, depth of maximum and size at maximum can be applied in the analysis of showers initiated by primary cosmic rays.
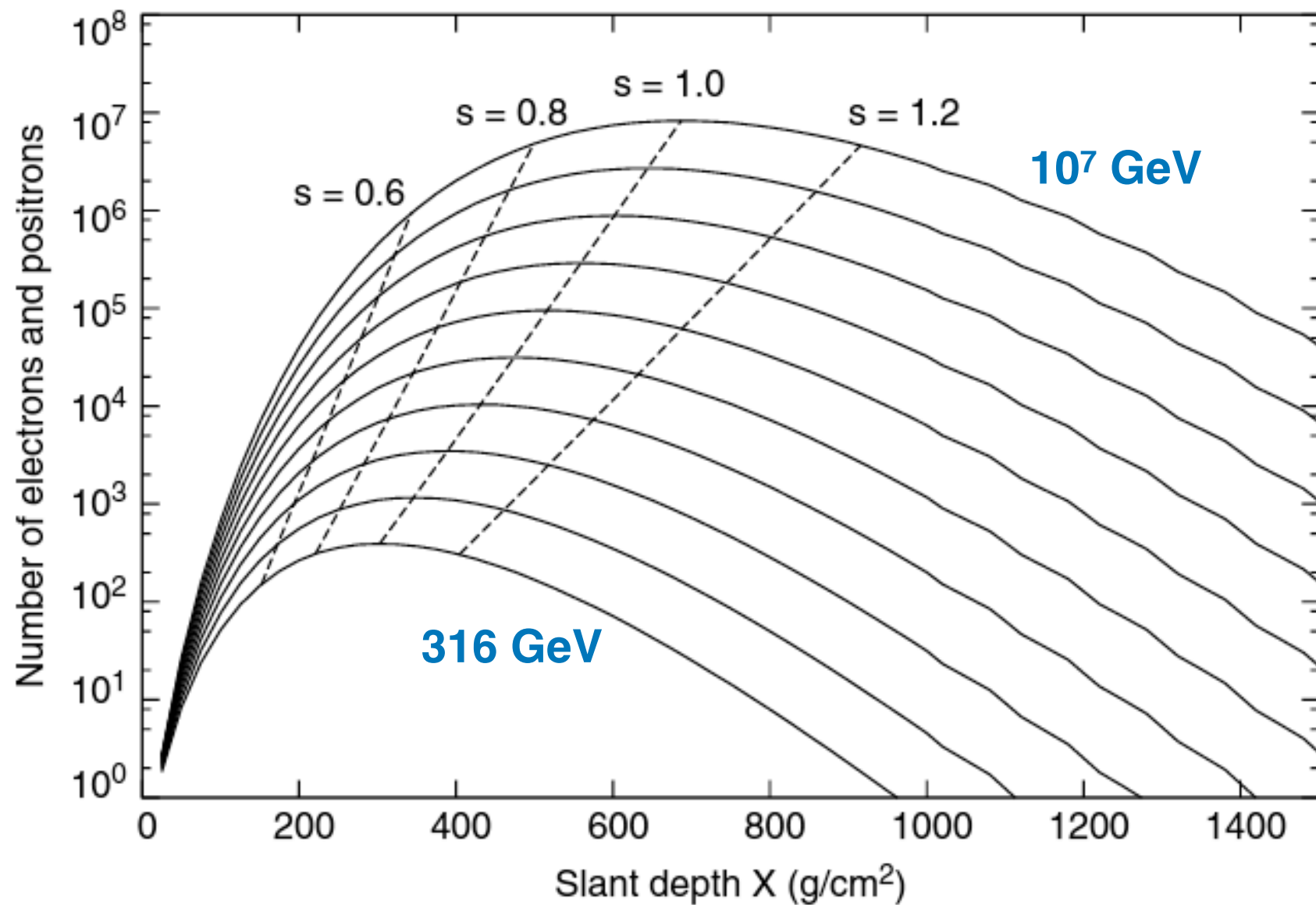
Figure 15.2 Shower size as a function of slant depth for photon-initiated showers in half-decade intervals of primary energy from 316 GeV (lowest curve) to 10^7 GeV (highest curve). The dashed lines trace the locus of size at specific shower ages across the same range of energies.

15.4 Fluctuations

For a given primary energy, fluctuations in the size of a shower measured at a particular depth in the atmosphere arise both from fluctuations in starting point and from fluctuations in the way the shower develops. An incident photon interacts with probability $dP/P = -\sigma_0 dt$, so $P(t_1) = \sigma_0 \exp[-\sigma_0 t_1]$ is the distribution of starting points for photon-induced showers. For this distribution

$$\delta t = \sqrt{\langle t^2 \rangle - \langle t \rangle^2} = \frac{1}{\sigma_0} = \frac{9}{7}. \tag{15.31}$$

Since $N(t) \propto \exp[\lambda_1(s)t]$, a measure of the corresponding fluctuation in $\ln N$ is

$$\delta \ln N \sim \lambda_1(s)\delta t \sim \frac{9}{14}(s - 1 - 3\ln s). \tag{15.32}$$

Fluctuations in shower size are thus proportional to N and are smallest near shower maximum. For a 10^{15} eV γ-initiated shower at sea level, for example, $s \sim 1.4$ and $\delta N \sim 0.4\,N$. When development fluctuations are included the overall fluctuations are somewhat larger. In summary, fluctuations in a sample of showers of the same energy observed at the same slant depth are approximately log-normal, reflecting the multiplicative character of the cascade process. This is clearly a general property of the branching process that will also hold for hadron-initiated showers. Fluctuations in proton-initiated showers may be larger because the interaction lengths for protons and mesons in the shower are larger than the electromagnetic radiation length.

15.5 Lateral spread

To obtain the lateral distribution of the particles in a shower front, it is necessary to include not only the opening angles in pair production and bremsstrahlung, but also multiple Coulomb scattering. In fact, it is the latter that determines the characteristic size of the shower front. The lateral spread of an electromagnetic shower is determined by the Molière unit, r_1, the natural unit of lateral spread due to Coulomb scattering. For multiple Coulomb scattering (Nishimura, 1967) [500]

$$\langle \delta\theta^2 \rangle = \left(\frac{E_s}{E} \right)^2 \delta t, \tag{15.33}$$

where $E_s = m_e c^2 (4\pi/\alpha)^{1/2} \approx 21$ MeV. The Molière unit, which characterizes the spread of low-energy particles in a shower is

$$r_1 = \frac{E_s}{E_c} X_0 \approx 9.3 \text{ g/cm}^2, \tag{15.34}$$

which is 78 m at sea level.[4] For higher-energy particles the characteristic spread, $R_E \sim r_1 E_c/E$, is smaller.

For calculations of showers in three dimensions it is necessary to solve equations for $\pi(E, x, y, \theta_x, \theta_y, t)$. Approximate solutions obtained by Kamata & Nishimura (1958) [501] and by Greisen (1956) [499] are compared in the article in *Handbuch der Physik* by Nishimura (1967) [500]. Greisen's form of the lateral distribution of electrons is known as the NKG formula,

$$x f(x) \propto x^{s-1} (1 + x)^{s-4.5},$$ (15.35)

valid for shower age $1.0 \leqslant s \leqslant 1.4$. In the NKG formula, $x = r/r_1$, and the particle density at a perpendicular distance r from the shower core is

$$\rho_N(r, t) = \frac{N_e(t)}{r_1^2} f(x),$$ (15.36)

where $N_e(t)$ is the total number of particles in the shower at t radiation lengths. The normalization is defined so that

$$2\pi \int_0^\infty x f(x) \, dx = 1.$$ (15.37)

The correlation between shower age and shape of the lateral distribution implied by Eq. 15.35 has been used to correlate a fitted value of s for a shower with its stage of development. This is problematic since real showers have hadronic cores that continually feed the electromagnetic component through $\pi^0 \rightarrow 2\gamma$. In addition, Monte Carlo simulations of electromagnetic cascades in air find steeper lateral distributions than the NKG distribution [502] and [503]. Nevertheless, the general form of the NKG function, or modifications of it, have proved useful in fitting observed showers.
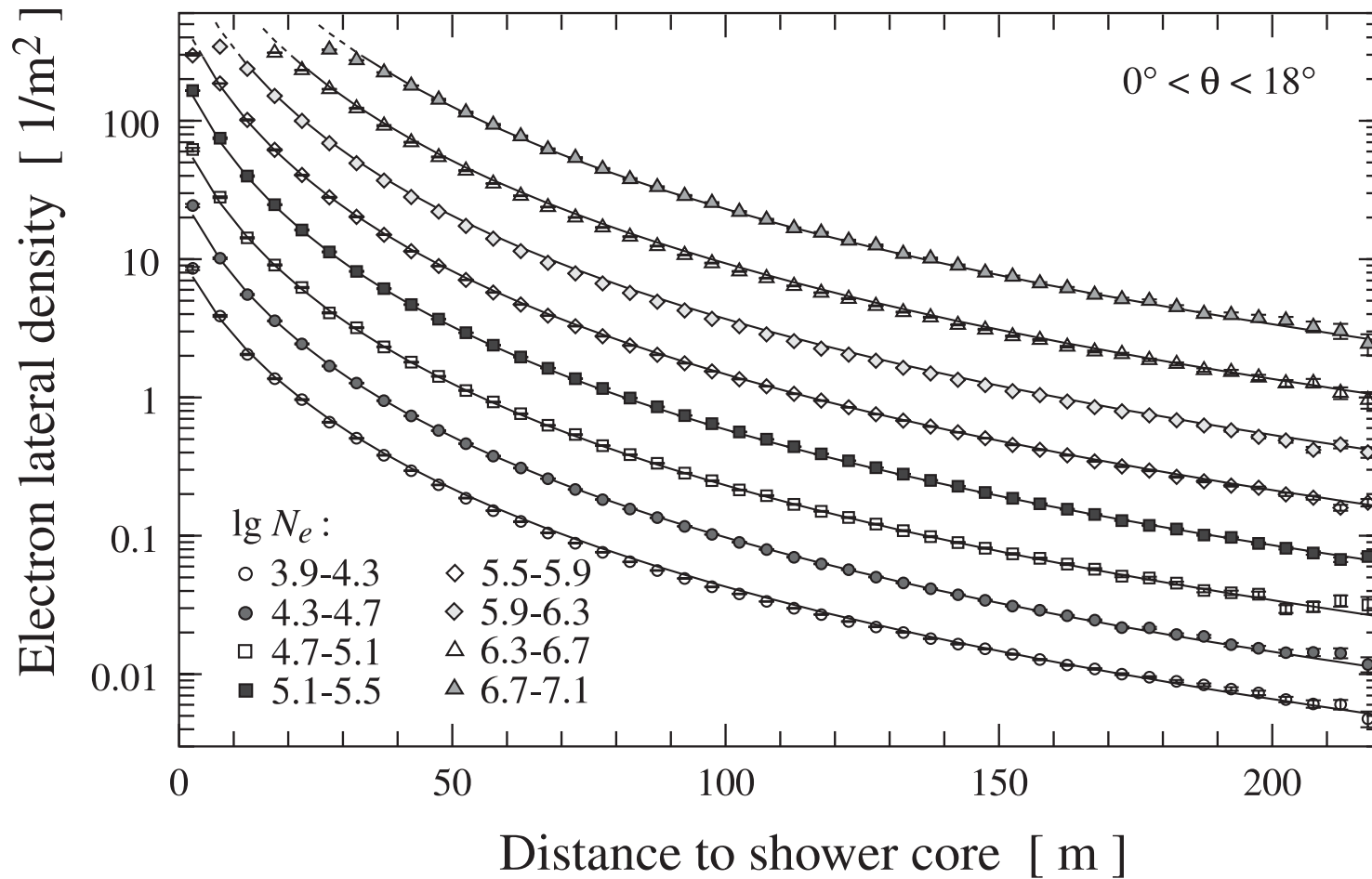
Fig. 2. Lateral distributions of electrons above a 5 MeV kinetic energy for zenith angles below 18°. The lines show NKG functions of fixed age parameter $s = 1.65$ but varying scale radius r_e (see the text).